



## **GOLD NANOPARTICLES PREPARATION AND DEPOSITION FOR ENHANCING THE SURFACE PROPERTIES AND OUTPUT OF TRIBOELECTRIC NANOGENERATOR**

**Deepak Anand\***, **Ashish Singh sambyal** and **Rakesh Vaid** Department of Electronics, University of Jammu, Jammu-180006, INDIA : [anand\\_a66@rediffmail.com](mailto:anand_a66@rediffmail.com)

### **ABSTRACT**

In this research paper, we present a very simple technique to create a triboelectric nanogenerator (TENG) composed of aluminum and PDMS (polydimethylsiloxane) layers to harness energy. The proposed TENG device can generate electricity through the process of triboelectrification. To improve the performance of the fabricated TENG, spherical gold nanoparticles were sprayed on the metal layer to increase the surface roughness of the layer. By applying force through Linear coil actuator, voltage and current of the device was also measured for various load resistances ranging from  $1\text{k}\Omega$  to  $100\text{k}\Omega$  generating a voltage of  $820.24\text{ mV}$ , current of value  $40.24\text{ }\mu\text{A}$  and an output power of  $8.99\text{ }\mu\text{W}$  respectively.

**KEYWORDS:** Triboelectric nanogenerator (TENG), Poly-dimethyl-siloxane (PDMS), Gold Nanoparticles (Au-NPs), Energy Harvesting

### **1. INTRODUCTION**

In the recent years the energy harvesting has drawn attention so as to supply sustained power for various electronic devices to be used in the fields of medical science, biosensors etc. Energy harvesting is used basically to convert waste energy that is available in our surroundings into useful electrical energy. In order to meet the rapidly increasing energy crisis and global warming [1-3], scientists and researchers are searching various sustainable, renewable and green energy sources so as to provide energy on a large scale. Various sources of energy like solar, wind, chemical, thermal and mechanical energy are available in abundance in nature and most of them goes waste because of their non- utilization. With the used of these energy sources as self-powered devices the use of battery can be limited/ reduces or devices without battery [4-7] can be manufactured. One of the most promising sources of energy that can be used as a clean and green energy source is mechanical energy. It finds its application in wireless sensors and in many portable /wearable electronic devices [8-12]. With the use of various mechanisms like piezoelectric, triboelectric, electromagnetic and electrostatic [13-22] the mechanical energy can be converted directly into electricity. With the use of piezoelectric and tribo electrification low frequency mechanical energy is converted into electricity that can be used for powering low voltage/ power electronic devices [23-29]. On the other hand vibration energy is available in abundance in nature, though the energy harvesting is very small but it finds its application in various portable and wearable electronic devices without the use of any external power source. In piezoelectric nanogenerators potential is generated with the application of force on the piezoelectric material which results in the flow of electrons through the external load [30-33]. The present day piezoelectric nanogenerators mainly depends upon various parameters like piezo charge co-efficient electro mechanical conversion factor (K), leakage current etc. which basically limits the use of these materials for energy harvesting. Thus the researchers mainly focus on triboelectric nanogenerators which are robust as well as cost effective. In general the triboelectric nanogenerators operations based on contact electrification and electrostatic induction [18, 26, and 27]. TENG finds its applications in wireless systems, portable, wearable electronics and in various self-powered systems [19, 29, 34, and 35] because of their low cost of operation, simple working, availability of variety of materials and higher performance. This device basically works on contact electrification and electrostatic induction [36-37]. Because of its limitations it is important to study

the surface morphology and choice of materials before fabricating a TENG device. Therefore a great effort has been made to propose a device that can provide electricity to be used for further applications. On the other hand, many studies have demonstrated the surface engineering of metal surfaces, such as the deposition of gold nanoparticles (Au-NPs) of various shapes and sizes. Gold is used in a variety of applications such as sensors because it is very robust against oxygen present in air and does not corrode or oxidize like other metals. It is also possible to easily fabricate gold nanoparticles of various shapes and sizes to generate large contact surface areas at room temperature and atmospheric pressure without using complex fabrication processes. Improvements in performance parameters are observed when gold nanoparticles are deposited on metal surfaces compared to metals without surface technology. Another advantage of using gold nanoparticles is that gold's robustness against oxygen does not require special protective packaging to protect the TENG device. Protective passivation is mandatory in various sensor applications, but not in the manufacture of this his TENG device as it collects waste energy from the environment. The surface stability of gold nanoparticles makes them suitable for various TENG applications. In this study, surface technology is presented for the first time by fabricating TENG devices. Deposition of gold nanoparticles (Au-NPs) on the surface of aluminum metal increases the contact area between the metal and the PDMS-based polymer layer, increasing the surface charge density. Pinch the device and apply force using your fingers or a static weight. Various parameters such as open-circuit voltage short-circuit current, and power varies as the applied force varies. From the results, it was observed that Au-NPs based his TENG performed well despite the fact that gold has a low triboelectric coefficient compared to other metals. Au-NPs based TENG fabricated in this way exhibit a high level of robustness even in very hot and humid environments.

## 2. PREPARATION AND DEPOSITION OF METAL LAYER

The substrate used in the manufacturing process is a 1.5" x 1" ITO coated glass that has first been properly cleaned using a soap solution. After the substrate is ultrasonically treated, it is treated at room temperature for about 15 minutes and then immersed in an IPA (isopropyl alcohol) solution. Finally, the substrate is dried using an air dryer. The substrate is now ready for the deposition process. First, a titanium metal layer of approximately 100 nm is deposited on the surface of the substrate. This essentially acts as a binder layer between the ITO-coated glass substrate and the aluminum layer. For the deposition of a 100 nm Ti layer, the average deposition rate is set to a value in the range of 30.2 A/s and the LT secondary current value is kept at the highest value of 62 amperes. For the deposition of 150 nm aluminum films, the average deposition rate is on the order of 17 A/s and 32 amperes for the deposition of aluminum. The water cooler has a pressure of 28 bars and a temperature value of 230 °C. This is done basically by the use of thermal vapor deposition technique by fixing various deposition parameters as depicted above. A schematic of the deposition process through thermal vapor deposition is as shown in Figure 1.

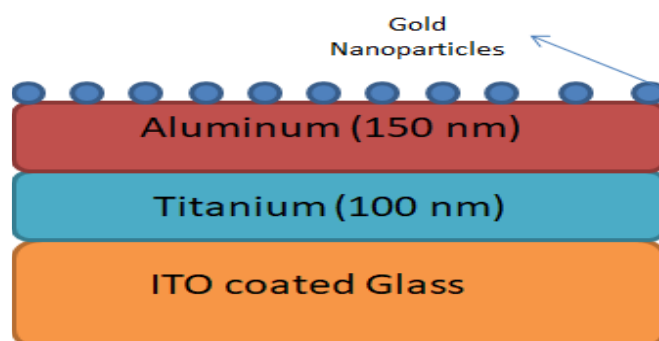


Fig. 1 Schematic diagram of deposition of metal layers by thermal vapor deposition.

### 3. PREPARATION AND DEPOSITION OF PDMS LAYER

In order to prepare the PDMS solution, thoroughly mix the Sylgard 184 elastomer and its curing agent in a 10:1 ratio. To further dilute the solution, add 1 mL of methyl chloride to the solution prepared above and keep the same solution under vacuum for approximately 30 min to remove air bubbles from the PDMS. A PDMS layer is deposited on the surface of the ITO-coated glass by a spin-coating technique, as shown in figure 2. Spin the spin coater at 2500 rpm for 40 s with an acceleration of 50 rpm to obtain a layer with a thickness of 8–10  $\mu\text{m}$ . The samples are then tempered in a muffle furnace at 150  $^{\circ}\text{C}$  for approximately 3 hours.

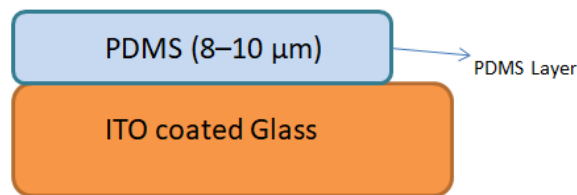


Fig. 2. Fabrication of PDMS Layer

### 4. SYNTHESIS AND DEPOSITION OF GOLD NANOPARTICLES (Au-NPs)

To prepare the seed solution, 2.4 mM gold chloride solution is mixed with 5 ml of distilled water. Also, mix together 2.4 mM trisodium citrate and ice-cold sodium borohydride. Finally, both solutions are mixed and stirred with a magnetic stirrer at 200 rpm for 10 min. To prepare the growth solution, CTAB (cetyltrimethylammonium bromide) at a concentration of 0.1 M is added to 20 ml of distilled/DI water. Again, add 2.24 mM gold chloride to pre-dissolved CTAB in distilled/DI water. Now add 600  $\mu\text{l}$  of the seed solution to the growth solution thus prepared, followed by stirring with a magnetic stirrer for about 10-15 minutes. The final step is to centrifuge the thus prepared solution to remove by-products or capping agents (sodium citrate). Therefore, the gold nanoparticles (Au-NPs) thus produced can be used for deposition on the surface of aluminum metal layers by spray pyrolysis.

### 5. FABRICATION OF TENG DEVICE AND ITS WORKING MECHANISM

The triboelectric nanogenerator thus fabricated consists of two layers. i) One layer consists of PDMS fabricated on an ITO-coated glass substrate and ii) the second layer is gold deposited on the surface of an aluminum layer fabricated on an ITO-coated glass substrate. In the fabricated device, the gold nanoparticles essentially serve a dual role. One is that it increases roughness when in contact with the PDMS layer and also acts as an electrode. Assemble the devices thus prepared using sponge as spacer and tape them to prevent delamination problems. The TENG devices thus prepared are then subjected to various forces (1–9 kgf) and also manually pushed to induce the phenomenon of contact separation. The electrical properties of the device were measured, including open circuit voltage, short circuit current, and output power at different values of applied weight/force. A schematic of the TENG device is shown below, where a 100 nm thick layer of titanium metal acts as a binder to bind a layer of aluminum (150 nm) to the surface of the substrate. Next, gold nanoparticles made by a sol-gel process are sprayed on the top layer to increase the surface roughness, so that better contact is formed between the two layers when superimposed, thereby increasing the surface charge density as well as the output performance.

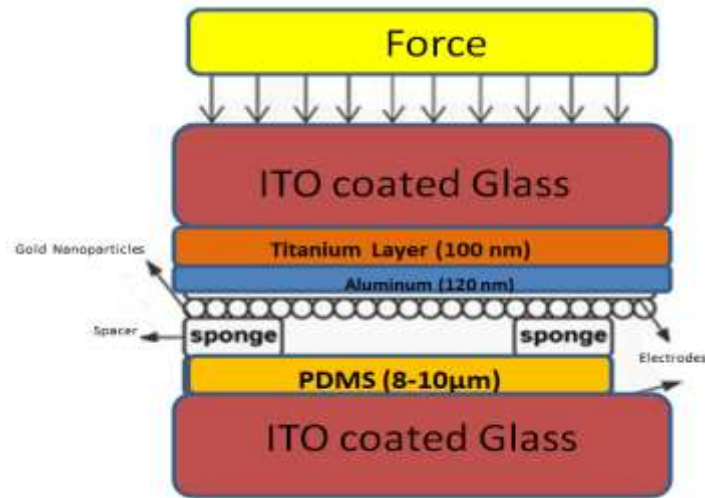


Fig. 3 Complete fabricated structure

The operating mechanism of the device thus manufactured is as shown in Fig.4. This device basically works with contact charging and electrostatic induction. In the initial stage, the friction layers are separated from each other by using a sponge as a spacer to separate the two layers by a distance 5mm distance as shown in fig. 4, so that the charge between the two surfaces is not created. When an external weight is placed on top of the top layer, the two friction layers come into contact with each other as shown in Fig. 4(a), generating a negative charge on the PDMS surface due to the roughness present. This negative charge caused a positive charge across the PDMS-ITO substrate interface due to charge neutrality. Removing the weight separates the two surfaces again, creating a potential gradient between the top and bottom electrodes, as shown in Fig. 4(b). Here, to reach the equilibrium state, electrons move from the bottom to the top electrode through an external circuit, as shown in Fig. 4(c). This process produces positive spikes in voltage and current readings. When the device is reloaded, the electrons move from the top electrode to the bottom electrode in order, and the equilibrium is lost. The electrons return to their original position (top to bottom of the electrode) until a new equilibrium is reached, creating a negative voltage and current spike to complete the entire cycle.

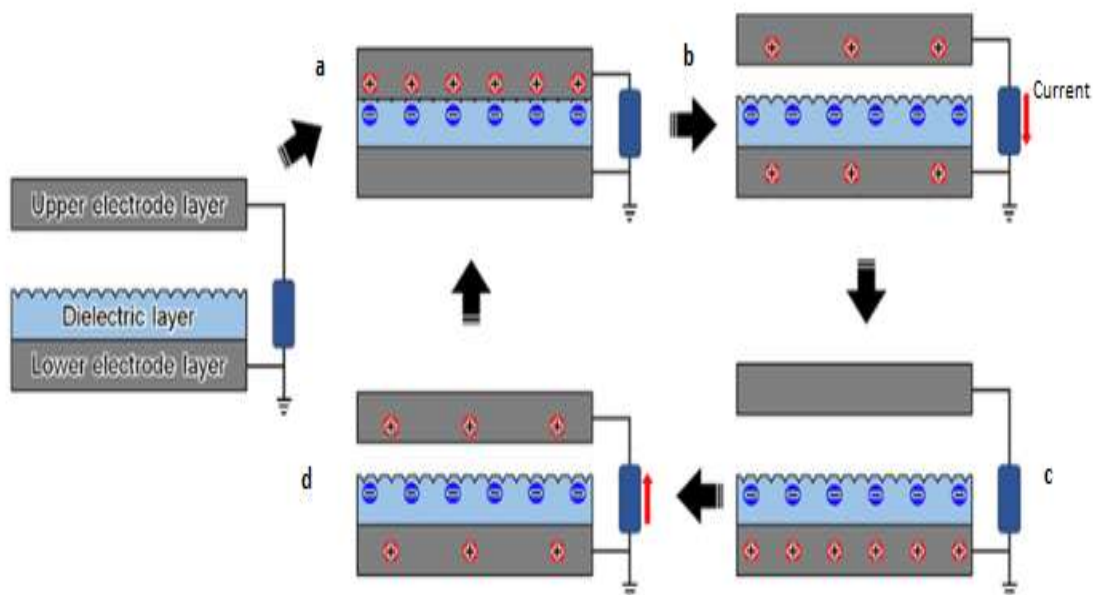


Fig. 4 Electricity generation process in TENG



- a) Contact of ITO and PDMS layer. b) Separation of layers by force reduction. c) Original state has triboelectric charges. d) Contact and movement of electrons

## 6. PHYSICAL/STRUCTURAL CHARACTERIZATIONS

The various physical /structural characterizations are as explained below:

### 6(a). Field Emission Scanning Electron Microscopy (FE-SEM)

The surface morphology of gold nanoparticles (Au-NPs) so prepared is characterized by the FESEM image as shown in figure below.

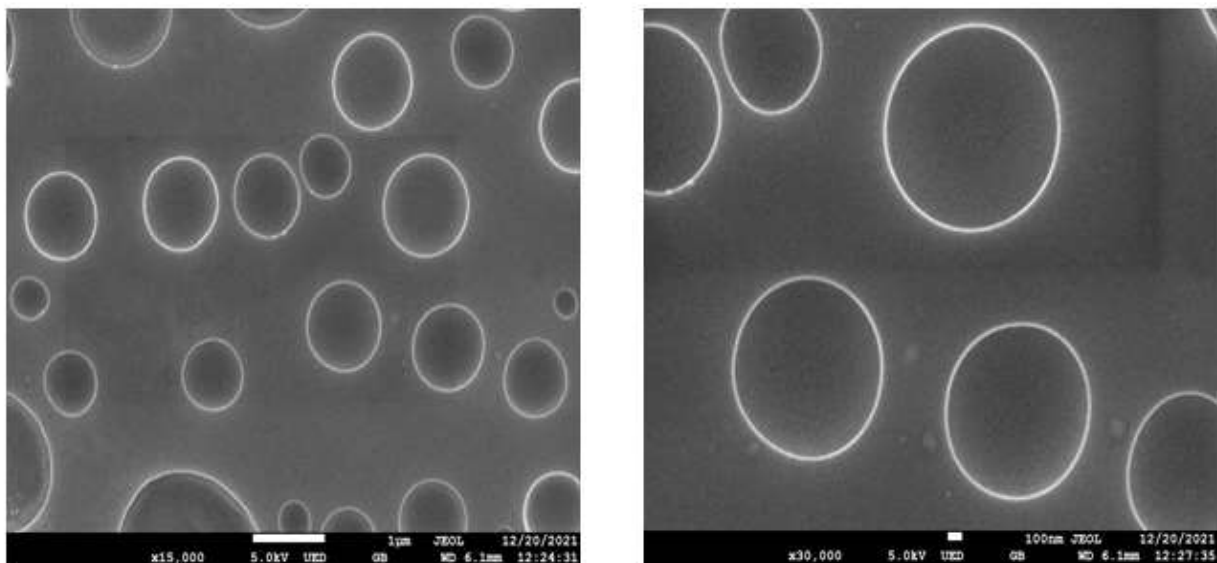


Fig. 5. FE-SEM images of the metal surface at different scales

From the obtained FESEM images, it was clarified that spherical gold nanoparticles precipitated on the surface of the aluminum metal used as the electrode, increasing the surface roughness of the upper surface and increasing the surface roughness. The contact area when two surfaces/layers come into contact with each other during the fabrication of a TENG device. The morphology of the PDMS surface is characterized FESEM (Field emission scanning electron microscopy) at different magnifications which clearly indicate cross linkages depicting that the polymer layer has been successfully deposited.

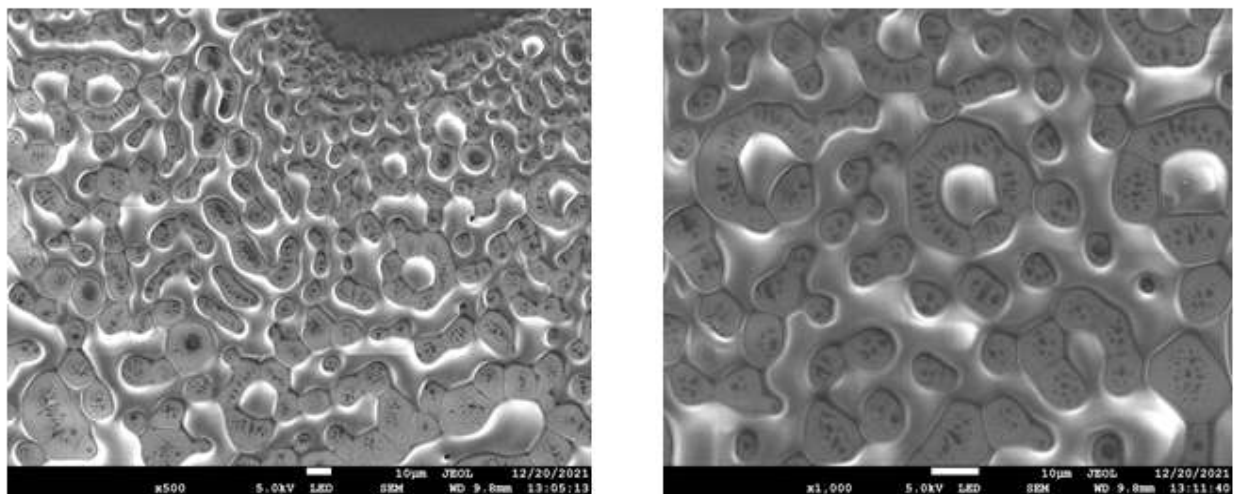


Fig. 6. FESEM images of PDMS of different magnifications

**6 (b). Energy Dispersive Spectroscopy (EDS)**

The elemental composition of the sample includes precipitation of titanium, aluminum-gold nanoparticles, and PDMS, as indicated by distinct peaks for each element, as shown in Figures 6 and 7. The sample is therefore ready for electrical characterization. EDS analysis of the elemental composition is shown in Table 1.

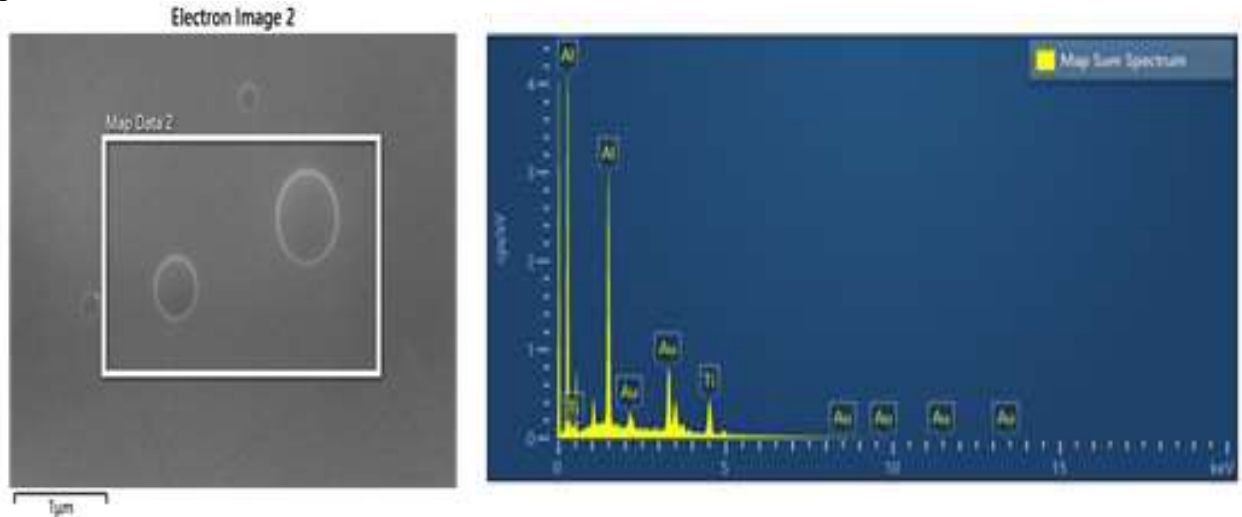


Fig. 7 EDS with unique peaks corresponding to different elements of metallic layers

TABLE 1 EDS ANALYSIS FOR ELEMENTAL COMPOSITION OF METAL LAYER

Element	Weight %	Atomic %
Titanium(Ti)	44.38	36.34
Aluminum(Al)	41.91	60.93
Gold(Au)	13.71	2.73
Total	100.00	100.00

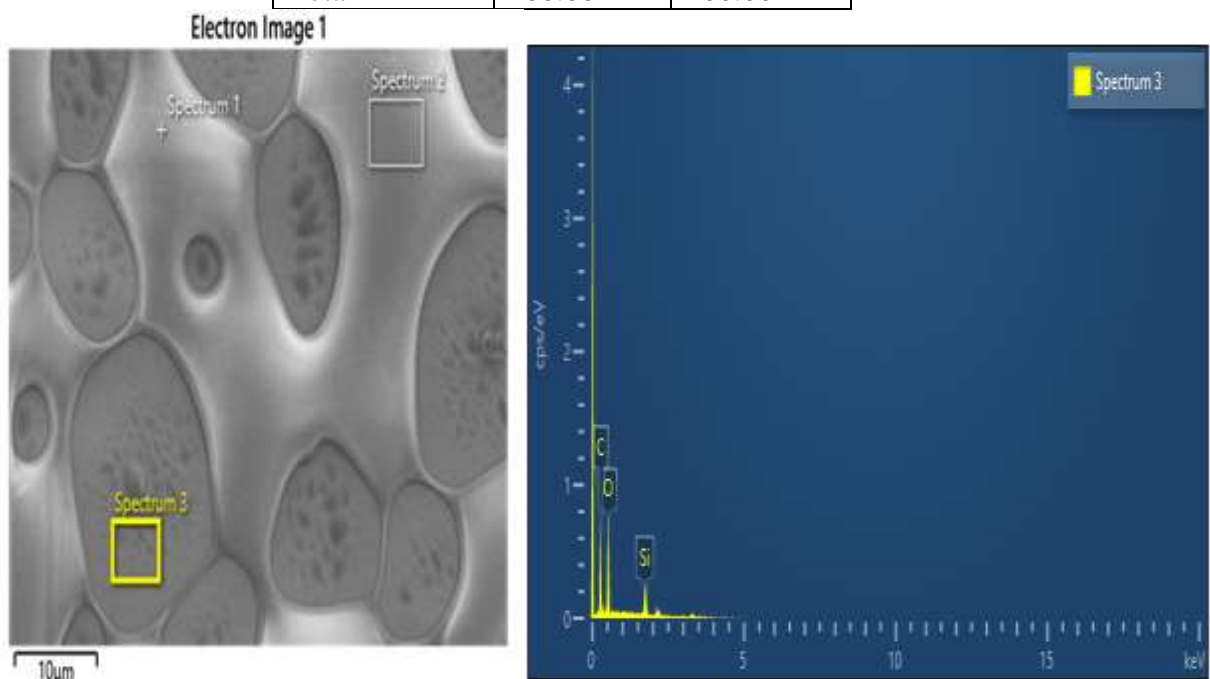


Fig.8. EDS with unique peaks corresponding to different elements of PDMS layer

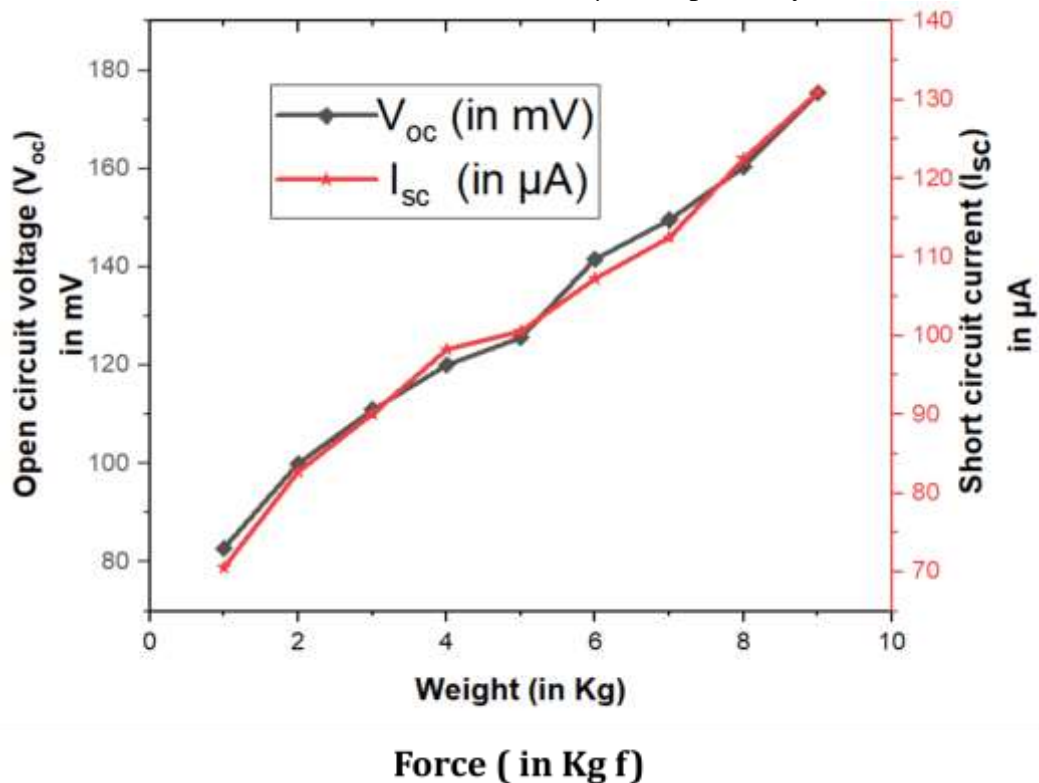
TABLE 2 EDS ANALYSIS FOR ELEMENTAL COMPOSITION OF PDMS LAYER

Element	Weight %	Atomic %
Carbon(C)	41.99	52.94
Oxygen(O)	38.75	36.67
Silicon(Si)	19.27	10.39
Total	100.00	100.00

## 7. ELECTRICAL CHARACTERIZATIONS

### 7 (a). Calculation of Open circuit voltage and Short circuit current

The output performance of the TENG fabricated in this way is examined with and without weights of different values, and the respective open circuit voltage and short circuit current are measured. The results obtained in this way are represented in graph 1. The graph shows that the open-circuit voltage and short-circuit current increase with increasing applied force, reaching a maximum open-circuit voltage of 175.45 mV and short-circuit current of 130.95 $\mu$ A, respectively.

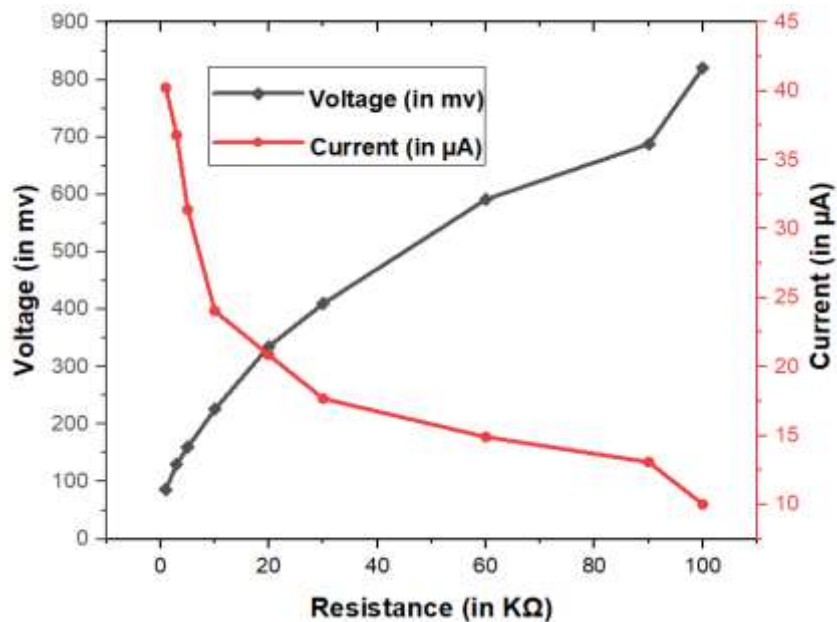


Graph 1 variation of open circuit voltage and short circuit current

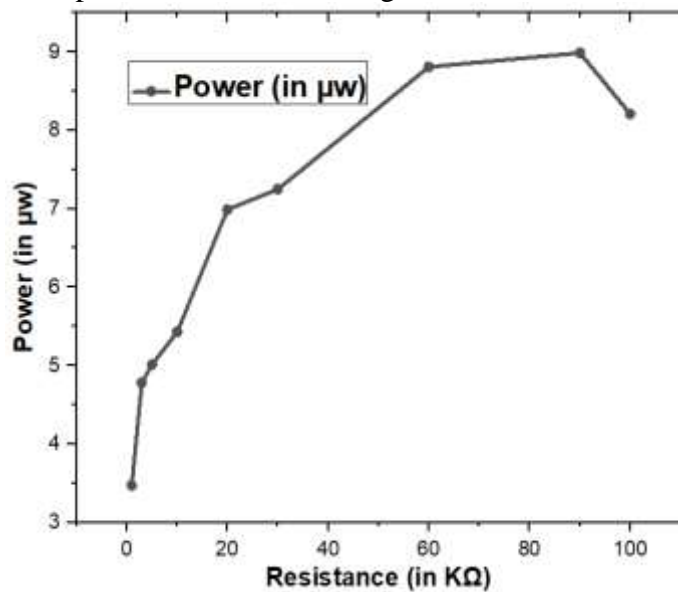
Graph1 shows the change in open circuit voltage and short circuit current as a function of applied weight. The applied force/weight increases the contact between the metal and polymer surfaces and increases the flow of charge carriers between the two surfaces, thereby enhancing the phenomenon of contact charging. Therefore, the increased weight and gradual contact separation between the surfaces creates a potential difference between the two triboelectric layers, which drives both the open-circuit voltage and the short-circuit current to a maximum value of 175.45 mV & 130.95  $\mu$ A respectively.

### 7 (b). Current – Voltage calculations under different load conditions

The effects of load resistance on voltage, current, and output power are presented in graphical form as shown below. The load resistance varies from 1K $\Omega$  to 100 K $\Omega$  and the maximum voltage value thus obtained applies to a load resistance of 100 K $\Omega$ , the maximum current corresponds to a minimum load of 1 K $\Omega$ , and the maximum output power obtained at a load resistance of 100 K $\Omega$ .



Graph 2 Variations of voltage and current with load



Graph 3 Variations of power with load

Graph 2 shows the output power of the metal polymer-based triboelectric nanogenerator under different external loads from 1 KΩ to 100 KΩ with different weight/applied force. As can be seen from the graph, the average voltage increases as the load increases, while the average current decreases due to resistive losses. At a maximum load of 100 KΩ, the maximum voltage achieved with this method is 820.24 mV and a maximum current of 40.24 μA is achieved with a minimum resistance of 1 KΩ. The variation in output power of manufactured TENG is expressed as a function of load resistance. A maximum power of 8.99 μW is achieved with a load resistance of 100 KΩ. Thus, the results so obtained suggest that aluminum and PDMS-based TENGs work efficiently when the load has a resistance of several kilo-ohms (KΩ).

## 8. CONCLUSION

In conclusion, it can be said that we have successfully fabricated gold nanoparticles and PDMS-based electro-rigid nanogenerator. The fabricate TENG device is therefore capable of converting mechanical energy applied in the form of force (N) through a linear voice coil actuator in the form of





electrical output. The surface roughness due to the gold nanoparticles plays an important role in generating the peak power of  $8.99 \mu\text{W}$ . Although the device produces very low power output, it has clearly demonstrated that power output can be achieved using random mechanical energy. However, with the control of various parameters such as photolithography, surface roughness, gap spacing, the output parameters can be increased and even with the use of flexible substrates, Flexible TENGs could be manufactured, which could lead to an upgraded version of the TENG that could find application in portable electronics and thus generate large output power so that the device could be used for commercial purposes.

**Acknowledgement:** The author Deepak Anand and Ashish Singh Sambyal organized the concept of this research paper and would like to thank Prof. Rakesh Vaid for supervising the project. All the authors read and approved the final manuscript.

### References

1. Omer, A.M.; The energy crisis, the role of renewable and global warming. *Greener journal of Environment management and public safety*. 1(1), 38-70 (2012).
2. Special issue on harnessing materials for energy. *MRS Bulletin*. 33(4), 261 (2008).
3. Wang, Z.L.; Towards self-powered nanosystems: from nanogenerators to nanopiezotronics. *Advanced Functional Materials*. 18, 3553–3567 (2008).
4. Tian, B., Zheng, X., Kempa, T.J., Fang, Y., Yu, N., Yu, G., Huang, J., Lieber, C.M.; Coaxial silicon nanowires as solar cells and nanoelectronic power sources. *Nature*. 449, 885–889 (2007).
5. Poudel, B., Hao, Q., Ma, Y., Lan, Y., Minnich, A., Yu, B., Yan, X., Wang, D., Muto, A., Vashaee, D., Chen, X., Liu, J., Dresselhaus, M.S., Chen, G., Ren, Z.; High-thermoelectric performance of nanostructured bismuth antimony telluride bulk alloys. *Science*. 320, 634–638 (2008).
6. Shao, Z., Haile S.M., Ahn, J., Ronney, P.D., Zhan, Z., Barnett, S.A.; A thermally self-sustained micro solid-oxide fuel-cell stack with high power density. *Nature*. 435, 795–798 (2005).
7. Wang, Z.L., Song, J.H.; Piezoelectric nanogenerators based on zinc oxide nanowire arrays. *Science*. 312, 242–246 (2006).
8. Wang, Z.L.; Self-powered nanosensors and nanosystems. *Advanced Materials*. 24, 280–285 (2011).
9. Mitcheson, P.D., Yeatman, E.M., Rao, G.K., Holmes, A.S., Green, T.C.; Energy harvesting from human and machine motion for wireless electronic devices. *Proceeding of the IEEE*. 96, 1457–1486 (2008).
10. Paradiso, J.A., Starner, T.; Energy scavenging for mobile and wireless electronics. *Pervasive Computing*. 4, 18–27 (2005).
11. Rogers, J.A., Huang, Y.G.; A curvy stretchy future for electronics. *Proceedings of the National Academy of Sciences*. 106, 10875–10876 (2009).
12. Kim, D.H., Lu, N., Ma, R., Kim, Y.S., Kim, R.H., Wang, S., Wu, J., Won, S.M., Tao, H., Islam, A., Yu, K.J., Kim, T., Chowdhury, R., Ying, M., Xu, L., Li, M., Chung, H.J., Keum, H., McCormick, M., Liu, P., Zhang, Y.W., Omenetto, F.G., Huang, Y., Coleman, T., Rogers, J.A.; Epidermal electronics *Science*. 333, 838–843 (2011).
13. Qin, Y., Wang, X., Wang, Z.L.; Microfibre–nanowire hybrid structure for energy scavenging. *Nature*. 451, 809–813 (2008).
14. Saravanakumar, B., Mohan, R., Thiyagarajan, K., Kim, S.J.; Fabrication of a ZnO nanogenerator for eco-friendly biomechanical energy harvesting. *RSC Advances*. 3, 16646–16656 (2013).
15. Saravanakumar, B., Kim, S.J.; Growth of 2D ZnO nanowall for energy harvesting application. *The Journal of Physical Chemistry C*. 118, 8831–8836 (2014).
16. Beeby, S.P., Torah, R.N., Tudor, M.J., Glynne-Jones, P., O'Donnell, T., Saha, C.R., Roy, S.A.; micro electromagnetic generator for vibration energy harvesting. *Journal of Micromechanics and Microengineering*. 17, 1257–1265 (2007).
17. Mitcheson, P.D., Miao, P., Stark, B.H., Yeatman, E.M., Holmes, A.S., Green, T.C.; MEMS



- electrostatic micropower generator for low frequency operation. *Sensors and Actuators A: Physical*. 115, 523–529 (2004).
18. Fan, F., Tian, Z., Wang, Z.L.; Flexible triboelectric generator. *Nano Energy*. 1, 328–334 (2012).
  19. Wang, S., Lin, L., Wang, Z.L.; Nanoscale triboelectric effect enabled energy conversion for sustainably powering portable electronics. *Nano Letters*. 12, 6339–6346 (2012).
  20. Cikim, T., Gozuasik, D., Kosar, A.; Power reclamation efficiency of a miniature energy-harvesting device using external fluid flows. *International Journal Energy Research*. 38, 1318–1330 (2014).
  21. Okamoto, H., Suzuki, T., Mori, K., Cao, Z., Onuki, T., Kuwano, H.; The advantages and potential of electret based vibration-driven micro energy harvesters. *International Journal Energy Research*. 33, 1180–1190 (2009).
  22. Silletto, M.N., Yoon, S.J., Arakawa, K.; Piezoelectric cable macro-fiber composites for use in energy harvesting. *International Journal Energy Research*. 39, 120–127 (2015).
  23. Chen, C.Y., Liu, T.H., Zhou, Y., Zhang, Y., Chueh, Y.L., Chu, Y.H., He, J.H., Wang, Z.L.; Electricity generation based on vertically aligned  $\text{PbZr}_{0.2}\text{Ti}_{0.8}\text{O}_3$  nanowire arrays. *Nano Energy*. 1, 424–428 (2012).
  24. Xu, S.Y., Poirier, G., Yao, N.; Fabrication and piezoelectric property of PMN-PT nanofibers. *Nano Energy*. 1, 602–607 (2012).
  25. Chen, X., Xu, S.Y., Yao, N., Shi, Y.; 1.6 V nanogenerator for mechanical energy harvesting using PZT nanofibers. *Nano Letters*. 10, 2133–2137 (2012).
  26. Fan, F.R., Lin, L., Zhu, G., Wu, W., Zhang, R., Wang, Z.L.; Transparent triboelectric nanogenerators and self-powered pressure sensors based on micropatterned plastic films. *Nano Letters*. 12, 3109–3114 (2012).
  27. Zhu, G., Pan, C.F., Guo, W.X., Chen, C.Y., Zhou, Y.S., Yu, R.M., Wang, Z.L.; Triboelectric-generator driven pulse electrodeposition for micropatterning. *Nano Letters*. 12, 4960–4965 (2012).
  28. Hu, Y.F., Zhang, Y., Xu, C., Zhu, G., Wang, Z.L.; High-output nanogenerator by rational unipolar assembly of conical nanowires and its application for driving a small liquid crystal display. *Nano Letter*. 10, 5025–5031 (2010).
  29. Zhong, J.W., Zhang, Q., Fan, F.R., Zhang, Y., Wang, S.H., Hu, B., Wang, Z.L., Zhou, J.; Finger typing driven triboelectric nanogenerator and its use for instantaneously lighting up LEDs. *Nano Energy*. 2, 491–497 (2012).
  30. Lee, S., Hinchet, R., Lee, Y., Yang, Y., Lin, Z.H., Ardila, G., Montès, L., Mouis, M., Wang, Z.L.; Ultra thin nanogenerators as self-powered/active skin sensors for tracking eye ball motion. *Advanced Functional Materials*. 24, 1163–1168 (2014).
  31. Park, K.I., Son, J.H., Hwang, G.T., Jeong, C.K., Ryu, J., Koo, M., Choi, I., Lee, S.H., Byun, M., Wang, Z.L., Lee, K.J.; Highly efficient, flexible piezoelectric PZT thin film nanogenerator on plastic substrates. *Advanced Functional Materials*. 26, 2514–2520 (2014).
  32. Saravanakumar, B., Soyoon, S., Kim, S.J.; Self-powered pH sensor based on a flexible organic-inorganic hybrid composite nanogenerator. *ACS Applied Materials & Interfaces*. 6, 13716–13723 (2014).
  33. Lin, Z.H., Yang, Y., Wu, J.M., Liu, Y., Zhang, F., Wang, Z.L.;  $\text{BaTiO}_3$  nanotubes based flexible and transparent nanogenerators. *Journal of Physical Chemical Letters*. 3, 3599–3604 (2012).
  34. Zhang, X.S., Han, M.D., Wang, R.X., Zhu, F.Y., Li, Z.H., Wang, W., Zhang, H.X.; Frequency-multiplication high output triboelectric nanogenerator for sustainably powering biomedical microsystems. *Nano Letters*. 13, 1168–1172 (2013).
  35. Lin, Z.H., Zhu, G., Zhou, Y.S., Yang, Y., Bai, P., Chen, J., Wang, Z.L.; Water-solid surface contact electrification and its use for harvesting liquid wave energy. *Angewandte Chemie International Edition*. 125, 12777–12781 (2013).
  36. Lin, Z.H., Zhu, G., Zhou, Y.S., Yang, Y., Bai, P., Chen, J., Wang, Z.L.; A self-powered triboelectric nano sensor for mercury ion detection. *Angewandte Chemie International Edition*. 52, 5065–5069 (2013).
  37. Zhu, G., Lin, Z.H., Jing, Q., Bai, P., Pan, C., Yan, Y., Zhou, Y., Wang, Z.L.; Toward large-scale energy harvesting by a nanoparticle-enhanced triboelectric nanogenerator. *Nano Letter*. 13, 847–853 (2013).